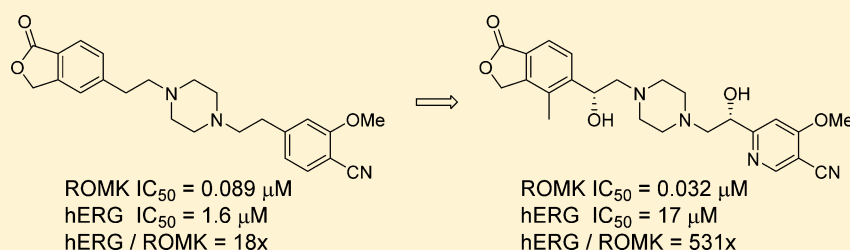


## Discovery of a Potent and Selective ROMK Inhibitor with Pharmacokinetic Properties Suitable for Preclinical Evaluation

Shawn P. Walsh,<sup>\*,†</sup> Aurash Shahripour,<sup>†</sup> Haifeng Tang,<sup>†</sup> Nardos Teumelsan,<sup>†</sup> Jessica Frie,<sup>†</sup> Yuping Zhu,<sup>†</sup> Birgit T. Priest,<sup>‡</sup> Andrew M. Swensen,<sup>‡</sup> Jessica Liu,<sup>‡</sup> Michael Margulis,<sup>‡</sup> Richard Visconti,<sup>‡</sup> Adam Weinglass,<sup>‡</sup> John P. Felix,<sup>‡</sup> Richard M. Brochu,<sup>‡</sup> Timothy Bailey,<sup>‡</sup> Brande Thomas-Fowlkes,<sup>‡</sup> Magdalena Alonso-Galicia,<sup>§</sup> Xiaoyan Zhou,<sup>§</sup> Lee-Yuh Pai,<sup>§</sup> Aaron Corona,<sup>§</sup> Caryn Hampton,<sup>§</sup> Melba Hernandez,<sup>§</sup> Ross Bentley,<sup>§</sup> Jing Chen,<sup>§</sup> Kashmira Shah,<sup>§</sup> Joseph Metzger,<sup>§</sup> Michael Forrest,<sup>§</sup> Karen Owens,<sup>||</sup> Vincent Tong,<sup>||</sup> Sookhee Ha,<sup>⊥</sup> Sophie Roy,<sup>§</sup> Gregory J. Kaczorowski,<sup>‡</sup> Lihu Yang,<sup>†</sup> Emma Parmee,<sup>†</sup> Maria L. Garcia,<sup>‡</sup> Kathleen Sullivan,<sup>§</sup> and Alexander Pasternak<sup>†</sup>

<sup>†</sup>Discovery Chemistry, <sup>‡</sup>Department of Pharmacology, <sup>§</sup>Department of Cardiometabolic Diseases, <sup>||</sup>Pharmacokinetic, Pharmacodynamics and Drug Metabolism, <sup>⊥</sup>Department of Chemistry Modeling and Informatics, Merck Research Laboratories, Kenilworth, New Jersey 07033, United States

### S Supporting Information



**ABSTRACT:** A new subseries of ROMK inhibitors exemplified by **28** has been developed from the initial screening hit **1**. The excellent selectivity for ROMK inhibition over related ion channels and pharmacokinetic properties across preclinical species support further preclinical evaluation of **28** as a new mechanism diuretic. Robust pharmacodynamic effects in both SD rats and dogs have been demonstrated.

**KEYWORDS:** ROMK, hypertension, heart failure, diuresis, natriuresis

Diuretics represent an important class of therapeutics for the treatment of human diseases. Thiazide diuretics, such as hydrochlorothiazide (HCTZ), represent first line therapy for uncomplicated hypertension; either alone or in combination with other agents.<sup>1</sup> Loop diuretics, such as furosemide, are indicated for the treatment of acute pulmonary edema and chronic heart failure.<sup>2</sup> Approved diuretics are not without their limitations, however. The thiazide diuretics, for example, are associated with hypokalemia (serum potassium <3.5 mEq/L) and elevation in fasting glucose, side effects that can be dose limiting. Common dose-dependent adverse reactions associated with loop diuretics include hyponatremia, hypokalemia, hypomagnesaemia, and dehydration, thus requiring careful electrolyte monitoring in patients.<sup>2</sup> Another drawback of loop diuretics is their short human half-lives (i.e., furosemide human half-life ~2 h), which are associated with robust initial diuretic responses (impacting tolerability) followed by rebound effects; short half-lives may also be responsible for the inferior blood pressure efficacy of loop diuretics compared to longer half-life thiazide diuretics.<sup>3</sup> Despite the established importance of these therapies and the opportunity for improvement over existing

therapeutics, no new diuretics have been disclosed to be in development.

Recent efforts in our laboratory aimed at the discovery of new mechanism diuretics have focused on the development of selective inhibitors for the Renal Outer Medullary Potassium Channel (ROMK, Kir1.1, encoded by *KCNJ1*).<sup>4,5</sup> This inward rectifying potassium channel is expressed at the apical membrane of epithelial cells lining two segments of the nephron: the thick ascending loop of Henle (TALH) and the cortical collecting duct (CCD).<sup>6</sup> At the TALH, ROMK facilitates potassium recycling across the luminal membrane, which is necessary for the proper function of the furosemide-sensitive Na<sup>+</sup>/K<sup>+</sup>/2Cl<sup>-</sup> cotransporter, the rate-determining step for sodium reuptake in this part of the nephron. At the CCD, ROMK provides a route for potassium secretion that is tightly coupled to sodium uptake through the amiloride-sensitive epithelial sodium channel.<sup>7,8</sup> Bartter's syndrome type II patients (*KCNJ1* homozygotes) lack functional ROMK expression and have a phenotype characterized by renal

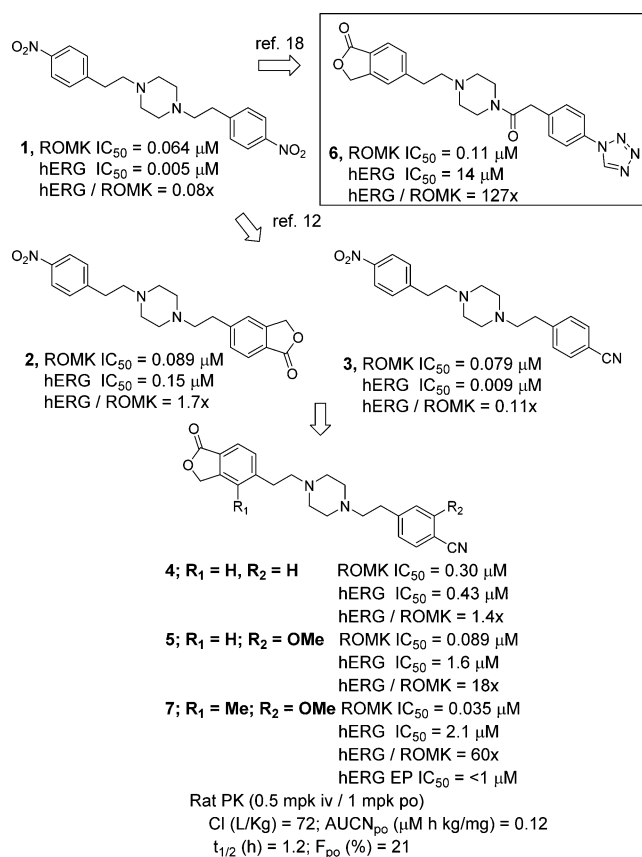
Received: December 30, 2014

Accepted: May 7, 2015

Published: May 7, 2015

salt wasting, hypotension, and mild hypokalemia.<sup>9</sup> A similar phenotype has been reported from studies with the ROMK knockout mice.<sup>9,10</sup> In addition, KCNJ1 heterozygote carriers from the Framingham Heart Study exhibited reduced blood pressure and a reduced risk of hypertension at age 60 when compared with matched controls.<sup>11</sup> Taken together, the evidence suggests that selective inhibitors of ROMK should represent novel diuretic/natriuretic agents with reduced kaliuresis, opportunity for improved pharmacokinetic (PK) and pharmacodynamic (PD) properties, and potential utility in the treatment of hypertension<sup>12</sup> and heart failure.<sup>13,14</sup>

Small molecule inhibitors of ROMK were first described by Denton at Vanderbilt University<sup>15,16</sup> and subsequently by our own group.<sup>17,18</sup> The initial lead series in our laboratories remarkably resulted from isolation of a potent impurity **1** (Figure 1) present in an otherwise inactive high throughput screening hit.



**Figure 1.** Replacement of the two nitrophenyl groups in **1**.

Subsequent studies detailed the development of this initial hit into a distinct subseries of potent and selective ROMK inhibitors (**6**). This effort resulted in the first pharmacological proof-of-biology, confirming for the first time *in vivo* that small molecule ROMK inhibitors represent a new class of novel mechanism diuretics with reduced kaliuresis.<sup>19</sup> In this Letter, we will describe the parallel development of a piperazinyl diol series resulting in ROMK inhibitors with superior potency, selectivity, and preclinical PK properties suitable for further evaluation.

For all compounds listed, unless otherwise specified, ROMK potency was determined as previously described using a thallium flux functional assay<sup>20</sup> in HEK-293 cells stably expressing ROMK and binding potency. For the outward delayed rectifier potassium channel (Kv11.1, human ether-a-go-go-related gene, hERG),

potency was determined by measuring displacement of <sup>35</sup>S MK499 from HEK-293 cells stably expressing hERG.<sup>21,22</sup>

As previously reported,<sup>17</sup> our initial follow-up to **1** focused on replacement of the two nitro groups with an eye toward improved selectivity over hERG compared to ROMK. Differentiation of the ROMK potassium ion channel activity from the hERG potassium ion channel activity was viewed as crucial due to the association between hERG channel blockade *in vitro* with QTc prolongation and risk of cardiac arrhythmias seen with a broad range of drugs.<sup>23–26</sup> To this end, phthalide and cyano groups (**2** and **3**) were identified as effective single nitro group replacements, able to maintain similar ROMK inhibition to **1**.<sup>17</sup> As previously described, combination of these groups led to identification of **4**, which represents a >10-fold improvement in the hERG/ROMK ratio over the initial hit; further exploration of the structure–activity relationships (SARs) of substitutions on the cyano-phenyl ring resulted in **5**, a potent ROMK inhibitor, which for the first time in our series provided a useful level of selectivity over hERG (18-fold).

Following the SAR successfully applied in our acyl piperazine subseries,<sup>18</sup> incorporation of the optimal 4-methyl substitution on the phthalide ring of **5** generated compound **7** (Figure 1). This compound displayed potent ROMK inhibition (0.035 μM) with reduced binding potency for the hERG channel (2.1 μM), resulting in a 60-fold selectivity window. Unfortunately, when **7** was evaluated in a hERG electrophysiology (EP) assay the potency was found to be less than 1.0 μM. Additionally, PK evaluation in Sprague–Dawley (SD) rats revealed the compound to have high clearance, low oral exposure, and modest half-life. Nevertheless, **7** represented a potent ROMK inhibitor and an interesting starting point for further optimization.

We reasoned that structural modifications capable of attenuating the basicity of the piperazine moiety in **7** might lead to beneficial impact on both hERG selectivity and PK parameters. In addition, substitutions that could reduce lipophilicity might also provide benefit. To this end, we next explored substitution at the α and β carbons flanking the nitrogens of the central piperazine ring (Table 1). On the carbon adjacent to the phthalide phenyl ring, methyl and fluoro substitution (**8** and **9**) led to modest loss of ROMK potency,

**Table 1.** Benzylic Substitution Structure–Activity Relationship<sup>a</sup>

#	R1	R2	R3	R4	X	ROMK IC <sub>50</sub> (μM)	hERG IC <sub>50</sub> (μM)
8	Me	H	H	H	C	0.170	2.8
9	F	H	H	H	C	0.060	2.4
10	OH	H	H	H	C	0.12	9.0
11	OMe	H	H	H	C	0.11	9.0
12	OEt	H	H	H	C	0.22	3.5
13	H	Me	H	H	C	0.19	1.3
14	H	H	Me	H	C	0.15	1.1
15	H	H	Me	Me	C	0.30	1.2
16	H	H	OH	H	C	0.070	2.2
17	H	H	OH	H	N	0.049	6.4

<sup>a</sup>All compounds are racemic.

resulting in an overall erosion of the hERG selectivity. Hydroxy or methoxy substitution (**10** and **11**) also resulted in a modest loss of ROMK potency, but the corresponding loss of hERG potency resulted in an overall improvement in the selectivity margin (>150-fold in the case of **10**). Further increase in the size of the alkoxy substituent to ethyl (**12**), however, resulted in a loss in ROMK potency and hERG margin. On the 4-CN phenyl side of the molecule, methyl substitution adjacent to the piperazine and mono- or dimethyl substitution at the benzylic position (**13**, **14**, and **15**) resulted in modest loss of ROMK potency and hERG selectivity. However, hydroxyl substitution at the benzylic position (**16**) largely maintained the potency and selectivity present in **7**. Guided by hERG selectivity improvements observed upon heteroatom incorporation in our related acyl piperazine series,<sup>27</sup> we also prepared the pyridyl analogue **17**. In this case, the pyridyl leads to retention of ROMK potency with an increased hERG/ROMK ratio (130-fold).

Based on these results, **10**, **16** and **17** were selected for PK evaluation in SD rats (0.5 mpk iv and 2 mpk po; Table 2). All

Table 2. SD Rat PK Properties of **7**, **10**, **16**, and **17**<sup>a</sup>

	<b>7</b>	<b>10</b>	<b>16</b>	<b>17</b>
Cl (L/kg)	72	33	40	40
AUCN <sub>po</sub> (μM h kg/mg)	0.12	0.46	0.35	0.74
t <sub>1/2</sub> (h)	1.2	0.83	1.3	1.5
F <sub>po</sub> (%)	21	39	37	78

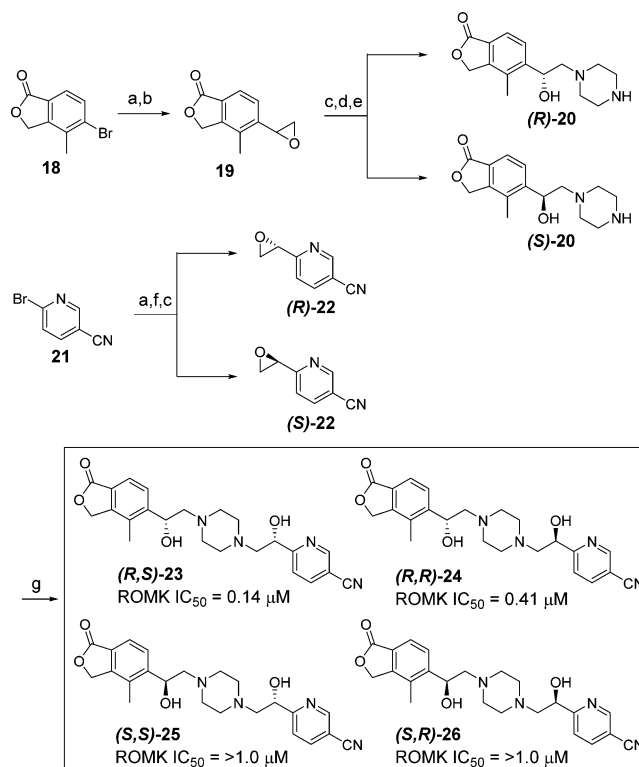
<sup>a</sup>All compounds are racemic.

three compounds showed modest improvement in clearance and oral exposure with little effect on half-life. Oral bioavailability was improved in all three cases; incorporation of the heterocyclic ring in **17** lead to the most significant effect.

Next we turned to combining the hydroxy substitution and to producing compounds as single enantiomers (Scheme 1). Suzuki cross coupling of **18** with the potassium vinyl trifluoroborate salt followed by *m*-chloroperbenzoic acid (mCPBA) epoxidation provided the racemic epoxide **19**. Chiral supercritical fluid chromatography (SFC) separation of the enantiomers followed by reaction of the individual epoxides with Boc-piperazine led to the individual hydroxy enantiomers.<sup>28</sup> We found that optimal selectivity for the terminal aminolysis of this and related styrene epoxides was achieved under thermal conditions in a microwave reactor in the absence of coordinating acid. Hydrolysis of the *t*-butyl carbamate was followed by basic workup to provide (*R*)- and (*S*)-**20** as their free amine bases. Synthesis of epoxides (*R*)- and (*S*)-**22** began with vinylation of the aryl bromide **21**; however, epoxidation of the resulting olefins with mCPBA led to competitive *N*-oxide formation. Alternatively, reaction with *N*-bromosuccinimide (NBS) and sodium hydroxide (NaOH) led to one-pot formation of the desired epoxides following *in situ* cyclization of the intermediate hydroxy bromides. Chiral SFC separation led to isolation of the individual epoxide enantiomers.<sup>29</sup> Reaction of the individual epoxides (*R*)- and (*S*)-**22** with (*R*)- and (*S*)-**20** provided the four individual products shown in Scheme 1.

Using the chemistry outlined in Scheme 1, a series of analogues was prepared to examine the effect of substitution on the 4-CN pyridyl ring (Table 3). Because the initial analogues made with (*S*)-**20** piperazine were substantially less potent, only (*R*)-**20** was used for subsequent analogues. Of the initial analogues, (*R,S*)-**23** provides the best combination of ROMK potency and hERG selectivity. In general, substitution in the

Scheme 1. Synthesis of Stereochemically Pure Diols **24**–**26**<sup>a</sup>

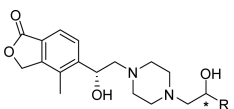


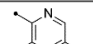
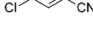
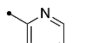
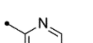
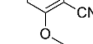
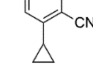
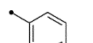
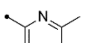
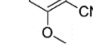
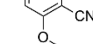
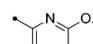
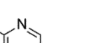
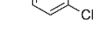
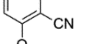
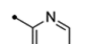
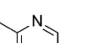

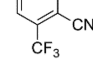
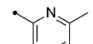
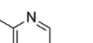
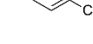
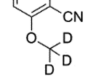
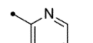
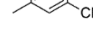
<sup>a</sup>Reagents and conditions: (a) potassium vinyltrifluoroborate, PdCl<sub>2</sub>(dppf)-CH<sub>2</sub>Cl<sub>2</sub>, triethylamine (TEA), ethanol (EtOH), 140 °C, MW; (b) mCPBA, CH<sub>2</sub>Cl<sub>2</sub>, 0 °C (40–70% yield, 2 steps); (c) ChiralPac AD-H SFC chromatography, 10% EtOH/CO<sub>2</sub>, flow rate 200 mL/min, 100 bar, 25 °C; (d) *N*-Boc-piperazine, EtOH, 150 °C, MW (50–90% yield); (e) (i) trifluoroacetic acid, CH<sub>2</sub>Cl<sub>2</sub>, rt, (ii) Na<sub>2</sub>CO<sub>3</sub> (aq) (85–90% yield); (f) NBS, H<sub>2</sub>O/*t*-butanol (2:1), 40 °C, then addition of NaOH at 0 °C (44–85% yield); (g) **20** + **22**, EtOH, 150 °C, MW (58–92% yield).

para- or meta-positions relative to the pyridine nitrogen resulted in compounds with improved ROMK potency, with the exception of the *p*-trifluoromethyl and *m*-chloro groups (**39**, **40**, **47**, and **48**). Of the ortho-substituents explored, only the methyl group (**35** and **36**) provided improved ROMK potency than (*R,S*)-**24**. Overall, the best balance of ROMK potency and hERG selectivity was achieved using the *p*-methoxy group ((*R,S*)-**28**). Deletion of the pyridyl nitrogen from (*R,R*)-**27** and (*R,S*)-**28** provided compounds with similar ROMK potency but reduced hERG selectivity (**29** and **30**), underscoring the importance of the heterocycle. No additivity was observed when combining the best para-substituent with the best ortho-substituent (OMe and Me, **43** and **44**). Finally, anticipating the *p*-methoxy group might undergo metabolism *in vivo*, we explored the size of the alkoxy group and incorporation of the trideutero-methoxy group (**45**, **46**, **49**, and **50**).

In addition to the Th flux and <sup>35</sup>S-MK499 assays, compounds were evaluated in ROMK and hERG EP assays (Table 4). There was good correlation of potency in both the ROMK and hERG EP assays, with three ROMK inhibitors identified with EP ratios of greater than 1000-fold. To understand how this level of *in vitro* selectivity translated *in vivo*, (*R,S*)-**28** was evaluated in anesthetized guinea pigs (*n* = 3). No significant change in QT interval was observed following IV infusion of (*R,S*)-**28** at 2 mpk (average peak unbound plasma concentration = 2.2 μM).

Table 3. Substitution around 5-CN pyridyl ring



Compound	R =	ROMK IC <sub>50</sub> (μM)	hERG IC <sub>50</sub> (μM)	hERG / ROMK	Compound	R =	ROMK IC <sub>50</sub> (μM)	hERG IC <sub>50</sub> (μM)	hERG / ROMK
( <i>R,S</i> )-23		0.14	28	128	39		0.50	5.7	43
( <i>R,R</i> )-24		0.41	ND	-	40		0.34	16	80
( <i>R,R</i> )-27 <sup>a</sup>		0.067	18	268	41		0.046	11	239
( <i>R,S</i> )-28 <sup>a</sup>		0.032	17	531	42		0.090	10	111
29		0.100	7.1	71	43		0.13	5.7	43
30		0.043	5.1	118	44		0.20	16	80
31		>3.0	ND	-	45		0.029	11	379
32		>3.0	ND	-	46		0.024	7.7	320
33		0.069	ND	-	47		0.85	4.8	5.6
34		0.061	ND	-	48		0.96	10	10
35		0.049	17	346	49		0.023	20	869
36		0.064	ND	-	50		0.016	21	1312
37		0.13	ND	239					
38		0.64	ND	111					

<sup>a</sup>Absolute configuration assigned using vibrational circular dichroism (VCD) spectroscopy. The other compounds obtained as single isomers, but with undetermined absolute stereochemistry.

Table 4. EP Evaluation of Selected Inhibitors

	6	23	28	35	41	46	50
ROMK EP IC <sub>50</sub> (nM)	64	18	27	12	54	40	13
hERG EP IC <sub>50</sub> (μM)	4.5	12	33	14	14	12	30
hERG/ROMK	70	667	1222	1166	254	300	2307

With several potent and selective ROMK inhibitors identified, we next turned to evaluating the PK profiles in SD rats (1 mpk iv and 2 mpk po; Table 5). All of the diol inhibitors evaluated demonstrated improvement in Cl, *t*<sub>1/2</sub>, oral exposure, and oral bioavailability versus the previously reported 6.

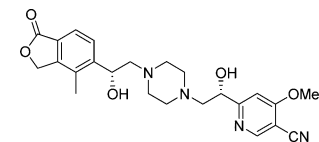
(*R,S*)-28 was further evaluated in functional assays for several related inward rectifying potassium channels (Kir 2.3, Kir2.1,

Table 5. SD Rat PK for Selected ROMK Inhibitors

	6	23	28	35	50
Cl (L/kg)	40	23	31	25	58
AUCN <sub>po</sub> (μM h kg/mg)	0.34	1.6	0.84	1.3	1.2
<i>t</i> <sub>1/2</sub> (h)	0.62	2.0	1.6	1.4	1.5
<i>F</i> <sub>po</sub> (%)	33	96	65	81	91

IC<sub>50</sub>s >50 μM; Kir4.1, Kir7.1 IC<sub>50</sub>s >10 μM) as well as the cardiac channels Nav 1.2 and Cav 2.1 (>30 μM) and found to have excellent selectivity for ROMK. (*R,S*)-28 was also evaluated for inhibition of a panel of CYPs (3A4, 2D6, 2C9; IC<sub>50</sub>s >50 μM) and found to have a signal only against 2C8 (IC<sub>50</sub> = 8.2 μM). Plasma protein binding (% free fraction) in rat and dog for (*R,S*)-28 was 43% and 83%, respectively, with excellent permeability (*P*<sub>app</sub> = 23). Finally, rat and dog ROMK Th flux IC<sub>50</sub>s for (*R,S*)-28 were found to be 0.014 and 0.042 μM, respectively.

(*R,S*)-28 was selected for further PK profiling in two additional species (dog and rhesus monkey; Table 6). The

Table 6. PK Properties of (*R,S*)-28 in Multiple Species


species	dose IV/PO (mpk)	CL (L/kg)	AUCN <sub>po</sub> (μM h kg/mg)	<i>t</i> <sub>1/2</sub> (h)	<i>F</i> <sub>po</sub> (%)
dog	0.5/1	5.6	5.6	5.9	84
rhesus	1/2	25	0.51	7.2	30

compound was found to have PK profiles across preclinical species consistent with an oral QD therapeutic. In addition, human half-life projection of (*R,S*)-28 based on observed preclinical PK in rat, dog, and rhesus monkeys by applying allometric scaling is estimated to be 10 h, significantly longer than the most commonly used loop diuretics furosemide and torsemide. This potentially provides a PK–PD advantage with regard to the peak diuretic effects associated with loop diuretics, by providing a reduction in peak-to-trough exposures.

(*R,S*)-28 was dosed orally in volume loaded SD rats at 0.3 and 1 mpk to assess its pharmacodynamic effects (Table 7).<sup>19</sup> (*R,S*)-

**Table 7. Acute 4 h Diuresis/Natriuresis of (*R,S*)-28 in SD Rats**

compound dose (mpk)	6 (3)	28 (0.3)	28 (1)	HCTZ (25)
diuresis <sup>a</sup>	2.3	2.3	2.8	2.1
natriuresis <sup>a</sup>	2.5	2.1	2.5	2.3
kaliuresis <sup>a</sup>	1.1	1.1	1.0	1.4

<sup>a</sup>Fold increase compared to vehicle; *n* = 5 per group.

28 demonstrated comparable efficacy at lower dose for diuresis and natriuresis over previously reported ROMK inhibitor 6 and HCTZ. Neither ROMK inhibitor induced statistically significant kaliuresis versus vehicle control in contrast to HCTZ (1.4-fold).

The diuretic and electrolyte excretion effects of (*R,S*)-28 were also evaluated following oral administration in female mongrel dogs to assess its PD effects (Table 8).<sup>30</sup> Robust dose-dependent increases in diuresis and natriuresis were observed over 24 h postdose, while kaliuretic response was not significantly changed versus vehicle control.

**Table 8. Twenty-Four Hour Diuresis/Natriuresis of (*R,S*)-28 in Dogs**

dose (mpk)	0.1	0.3	1	3	10
AUC (μM·h)	0.081	0.51	1.1	5.0	15
diuresis <sup>a</sup>	1.1	1.7	2.1	2.8	4.5
natriuresis <sup>a</sup>	1.0	1.5	1.6	1.5	2.6
kaliuresis <sup>a</sup>	1.0	0.88	0.60	0.78	1.0

<sup>a</sup>Fold increase compared to vehicle; *n* = 6 per group.

In summary, a new subseries of ROMK inhibitors exemplified by (*R,S*)-28 has been developed. Excellent selectivity for ROMK inhibition over related ion channels and PK properties of (*R,S*)-28 across preclinical species support continued evaluation of this compound as a new mechanism diuretic. Robust PD effects in both SD rats and dogs have been demonstrated. Translation of ROMK mediated diuresis effects into preclinical blood pressure lowering and further mechanistic studies will be the subject of future communications.

## ■ ASSOCIATED CONTENT

### Supporting Information

Synthesis and characterization data for compounds 7, (*R,S*)-23, (*R,R*)-27, (*R,S*)-28, 35, 41, 46, and 50. Additional details regarding assay correlation. The Supporting Information is available free of charge on the ACS Publications website at DOI: 10.1021/ml500440u.

## ■ AUTHOR INFORMATION

### Corresponding Author

\*E-mail: shawn\_walsh@merck.com.

## Notes

The authors declare no competing financial interest.

## ■ REFERENCES

- (1) Tamargo, J.; Segura, J.; Ruilope, L. M. Diuretics in the Treatment of Hypertension Part 1. Thiazide and Thiazide-like Diuretics. *Expert Opin. Pharmacother.* **2014**, *15* (4), 527.
- (2) Felker, G. M.; O'Connor, C. M.; Braunwald, E. Loop Diuretics in Acute Decompensated Heart Failure. *Circulation: Heart Failure* **2009**, *2*, 56.
- (3) Ellison, D. H. Diuretic Resistance: Physiology and Therapeutics. *Semin. Nephrol.* **1999**, *19* (6), 581–597.
- (4) Ho, K.; Nichols, C. G.; Lederer, W. J.; Lytton, J.; Vassilev, P. M.; Kanazirska, M. V.; Hebert, S. C. Cloning and Expression of an Inwardly Rectifying ATP-regulated Potassium Channel. *Nature* **1993**, *362*, 31.
- (5) Shuck, M. E.; Bock, J. H.; Benjamin, C. W.; Tsai, T. D.; Lee, K. S.; Slightom, J. L.; Bienkowski, M. J. Cloning and Characterization of Multiple Forms of the Human Kidney ROM-K Potassium Channel. *J. Biol. Chem.* **1994**, *269*, 24261.
- (6) Hebert, S. C.; Desir, G.; Giebisch, G.; Wang, W. Molecular Diversity and Regulation of Renal Potassium Channels. *Physiol. Rev.* **2005**, *85*, 319.
- (7) Reinalter, S. C.; Jeck, N.; Peters, M.; Seyberth, H. W. Pharmacotyping of Hypokalemic Salt-losing Disorder. *Acta Physiol. Scand.* **2004**, *181*, 513.
- (8) Wang, W. Renal Potassium Channels: Recent Development. *Curr. Opin. Nephrol. Hypertens.* **2004**, *13*, 549.
- (9) Ji, W.; Foo, J. N.; O'Roak, B. J.; Zhao, H.; Larson, M. G.; Simon, D. B.; Newton-Cheh, C.; State, M. W.; Levy, D.; Lifton, R. P. Rare Independent Mutations in Renal Salt Handling Genes Contribute to Blood Pressure Variation. *Nat. Genet.* **2008**, *40*, 592.
- (10) Lorenz, J. N.; Baird, N. R.; Judd, L. M.; Noonan, W. T.; Andringa, A.; Doetschman, T.; Manning, P. A.; Liu, L. H.; Miller, M. L.; Shull, G. E. Impaired Renal NaCl Absorption in Mice Lacking the ROMK Potassium Channel, a Model for Type II Bartter's Syndrome. *J. Biol. Chem.* **2002**, *277*, 37871.
- (11) Lu, M.; Wang, T.; Yan, Q.; Yang, X.; Dong, K.; Knepper, M. A.; Wang, W.; Giebisch, G.; Shull, G. E.; Hebert, S. C. Absence of Small Conductance K<sup>+</sup> Channel (SK) Activity on Apical Membranes of Thick Ascending Limb and Cortical Collecting Duct in ROMK (Bartter's) Mice. *J. Biol. Chem.* **2002**, *277*, 37881.
- (12) Tobin, M. D.; Timpson, N. J.; Wain, L. V.; Ring, S.; Jones, L. R.; Emmett, P. M.; Palmer, T. M.; Ness, A. R.; Samani, N. J.; Smith, G. D.; Burton, P. R. Common Variation in the WNK1 Gene and Blood Pressure in Childhood. *Hypertension* **2008**, *51*, 1658.
- (13) Lifton, R. P.; Gharavi, A. G.; Geller, D. S. Genetic Factors in the Pathogenesis of Primary (Essential) Hypertension. *Cell* **2001**, *104*, 545.
- (14) Garcia, M. L.; Kaczorowski, G. J. Targeting the Inward-Rectifier Potassium Channel ROMK in Cardiovascular Disease. *Curr. Opin. Pharmacology* **2014**, *15*, 1.
- (15) Lewis, L. M.; Bhawe, G.; Chauder, B. A.; Banerjee, S.; Lornsen, K. A.; Redha, R.; Fallen, K.; Lindsley, C. W.; Weaver, C. D.; Denton, J. S. High Throughput Screening Reveals a Small-molecule inhibitor of the Renal Outer Medullary Potassium Channel and Kir7.1. *Mol. Pharmacol.* **2009**, *1094*, 76.
- (16) Bhawe, G.; Chauder, B. A.; Liu, W.; Dawson, E. S.; Kadakia, R.; Nguyen, T. T.; Lewis, L. M.; Meiler, J.; Weaver, D. D.; Satlin, L. M.; Lindsley, C. W.; Denton, J. S. Development of a Selective Small-molecule Inhibitor of Kir<sub>1,1</sub>, the Renal Outer Medullary Potassium Channel. *Mol. Pharmacol.* **2011**, *79*, 42.
- (17) Tang, H.; Walsh, S. P.; Yan, Y.; de Jesus, R. K.; Shahripour, A.; Teumelsan, N.; Zhu, Y.; Ha, S.; Owens, K. A.; Thomas-Fowlkes, B. S.; Felix, J. P.; Liu, J.; Kohler, M.; Priest, B. T.; Bailey, T.; Brochu, R.; Alonso-Galicia, M.; Kaczorowski, G. J.; Roy, S.; Yang, L.; Mills, S. G.; Garcia, M. L.; Pasternak, A. Discovery of Selective Small Molecule ROMK Inhibitors as Potential New Mechanism Diuretics. *ACS Med. Chem. Lett.* **2012**, *3*, 367.
- (18) Tang, H.; de Jesus, R. K.; Walsh, S. P.; Zhu, Y.; Yan, Y.; Priest, B. T.; Swensen, A. M.; Alonso-Galicia, M.; Felix, J. P.; Brochu, R. M.;

Bailey, T.; Thomas-Fowlkes, B.; Zhou, X.; Pai, L.-Y.; Hampton, C.; Hernandez, M.; Owens, K.; Roy, S.; Kaczorowski, G. J.; Yang, L.; Garcia, M. L.; Pasternak, A. Discovery of a Novel Sub-Class of ROMK Channel Inhibitors Typified by 5-(2-(4-(2-(1H-Tetrazole-1-yl)phenyl)acetyl)-piperazin-1-yl)ethyl)isobenzofuran-13H-one. *Bioorg. Med. Chem. Lett.* **2013**, *23*, 5829.

(19) Garcia, M. L.; Priest, B. T.; Alonso-Galicia, M.; Zhou, X.; Felix, J. P.; Brochu, R. M.; Bailey, T.; Swensen, A.; Pai, L.-Y.; Xiao, J.; Hernandez, M.; Hoagland, K.; Owens, K.; Tang, H.; de Jesus, R.; Roy, S.; Kaczorowski, G. J.; Pasternak, A. Pharmacologic Inhibition of the Renal Outer Medullary Potassium Channel Causes Diuresis and Natriuresis in the absence of Kaliuresis. *J. Pharm. Exp. Ther.* **2014**, *348*, 153.

(20) Felix, J. P.; Priest, B. T.; Solly, S.; Bailey, T.; Brochu, R. M.; Liu, C. J.; Kohler, M. G.; Kiss, L.; Alonso-Galicia, M.; Tang, H.; Pasternak, A.; Kaczorowski, G. J.; Garcia, M. L. The Inward Rectifying Potassium Channel Kir1.1; Development of Functional Assays to Identify and Characterize Channel Inhibitors. *Assay Drug Dev. Technol.* **2012**, *10*, 417.

(21) Wang, J.; Della Penna, K.; Wang, H.; Karczewski, J.; Connolly, T. M.; Koblan, K. S.; Bennett, P. B.; Salata, J. J. Functional and Pharmacological Properties of Canine ERG Channels. *Am. J. Phys.* **2003**, *284*, 256.

(22) Further details regarding standard deviations and number of assay runs are available in the Supporting Information.

(23) Caverio, I.; Mestre, M.; Guillon, J.-M.; Crumb, W. Drugs that Prolong QT Interval as an Unwanted Effect; Assessing their Likelihood of Inducing Hazardous Cardiac Dysrhythmias. *Expert Opin. Pharmacother.* **2000**, *1*, 947.

(24) Sanguinetti, M. C.; Jiang, C.; Curran, M. E.; Keating, M. T. A Mechanistic Link Between an Inherited and Acquired Cardiac Arrhythmia; HERG Encodes the IKr Potassium Channel. *Cell* **1995**, *81*, 299 ..

(25) Fermini, B.; Fossa, A. A. Nat. Rev. The impact of Drug Induced QT Prolongation on Drug Discovery and Development. *Nat. Rev. Drug Discovery* **2003**, *2*, 439.

(26) Pearlstein, R.; Vaz, R.; Rampe, D. J. Understanding the Structure-activity Relationship of the Human Ether-a-go-go-related Gene Cardiac K<sup>+</sup> Channel. *J. Med. Chem.* **2006**, *49*, 4801.

(27) Full description of this related series will be the subject of another publication.

(28) The absolute stereochemistry of each enantiomer was inferred based on X-ray structure determination of a derivative made from (*R*)-**20** and by Mosher ester and Trost ester <sup>1</sup>H NMR analysis of a derivative made from the *t*-butyl carbamate of (*R*)-**21**.

(29) The absolute stereochemistry of each enantiomer was determined using vibrational circular dichroism (VCD).

(30) Description of the dog diuresis model will be included separately as part of a full pharmacology paper.